Diffusion and Spatial Correlations in Suspensions of Swimming Particles

Patrick T. Underhill, Juan P. Hernandez-Ortiz,* and Michael D. Graham†

Department of Chemical and Biological Engineering, University of Wisconsin-Madison, 1415 Engineering Drive, Madison, Wisconsin 53706, USA

(Received 4 October 2007; published 16 June 2008)

Populations of swimming micro-organisms produce fluid motions that lead to dramatically enhanced diffusion of tracer particles. Using simulations of suspensions of swimming particles in a periodic domain, we capture this effect and show that it depends qualitatively on the mode of swimming: swimmers ''pushed'' from behind by their flagella show greater enhancement than swimmers that are ''pulled'' from the front. The difference is manifested by an increase, that only occurs for pushers, of the diffusivity of passive tracers and the velocity correlation length with the size of the periodic domain. A physical argument supported by a mean field theory sheds light on the origin of these effects.

DOI: 10.1103/PhysRevLett.100.248101 PACS numbers: 87.17.Jj, 47.15.G−, 83.10.Rs

In the present Letter we consider the possibility of emergence of large scale fluid motion and enhanced fluid transport in populations of small swimming organisms. At the global scale, it has been suggested that swimming organisms such as krill can alter mixing in the oceans [1,2]. At the laboratory scale, experiments with suspensions of swimming cells have revealed characteristic swirls and jets much larger than a single cell, as well as causing increased diffusivity of tracer particles [3–7]. This enhanced diffusivity may have important consequences for how cells reach nutrients, as it indicates that the very act of swimming towards nutrients alters their distribution. The enhanced diffusivity has also been proposed as a scheme to improve transport in microfluidic devices [8] and might be exploited in microfluidic cell culture of motile organisms or cells.

The feedback between the motion of swimming particles and the fluid flow generated by that motion is thus very important. Nevertheless, in the literature on collective dynamics of self-propelled particles, this effect has received little attention. Most previous attempts to understand the collective motion of swimming micro-organisms fall into two broad categories: ''particle level'' approaches based on *ad hoc* interaction rules between the individual agents, e.g. [9], and continuum models of active suspensions based on phenomenological field equations [10–12]. The hydrodynamics of single swimming organisms at low Reynolds number have been studied for many years [13–15], and studies of hydrodynamic interactions (HI) have also been performed for pairs of swimmers [16–18]. However, only a small number of studies [19–24] have examined particle level models of *populations* of swimmers that include the fluid motion caused by the swimmers and its influence on transport. Hernandez-Ortiz *et al.* [19,20] developed a simple physical model of self-propelled particles, and performed simulations of them in a confined domain. Their work showed that multibody HI between self-propelled particles were sufficient to lead to fluid motions characteristic of those seen in experiments. Llopis and Pagonabarraga [21] performed simulations of self-propelled particles in two-dimensions, observing aggregates of swimming particles and a decrease of velocity with increasing volume fraction. Saintillan and Shelley [22] performed simulations of long, slender self-propelled rods propelled by an imposed shear stress on the surface of part of the rods. Their main result was that initially nematically ordered swimmers do not remain aligned except with very near neighbors. Pedley and co-workers [23,24] examined the rheology and random walk motion of semidilute suspensions of self-propelled spheres.

We consider here a suspension of N neutrally buoyant rodlike swimmers in a spatially periodic cubic fluid domain of side length L, in a concentration regime dilute enough that the dominant interactions between the particles arise from the fluid motions that they generate as they swim. Each swimmer has a characteristic length ℓ, and in isolation moves in a straight line with speed v_{is}. It is assumed that the Reynolds number $v_{is}L/\nu$ is much less than 1, where ν is the fluid kinematic viscosity. The concentration is given as an effective volume fraction $\phi_e = \pi N\ell^3/(6L^3)$—this would be the true volume fraction if the swimmers were spheres of diameter ℓ. To allow large populations ($>10^4$ swimmers) over long times, a simple model of each swimmer is adopted, following our previous work [19].

Each self-propelled particle is represented as two beads connected by a stiff spring with equilibrium length ℓ as shown in Fig. 1. The unit vector pointing along the axis from bead 1 to bead 2 is denoted $\mathbf{n}$. The propulsion is provided by a ''phantom flagellum'' that we do not treat explicitly, but only through its effect on the swimmer body and the fluid. This flagellum exerts a force $\mathbf{F}_f$ on bead 1 of the swimmer, and also exerts a force $-\mathbf{F}_f$ on the fluid. This force on the fluid occurs at the position of bead 1. With this model we can consider ''pushers'' or ''pullers'' depending on whether $\mathbf{F}_f$ is parallel or antiparallel to $\mathbf{n}$, respectively. A pusher sends fluid away from it fore and aft, with fluid moving toward its ''waist,'' and vice versa for a puller. A

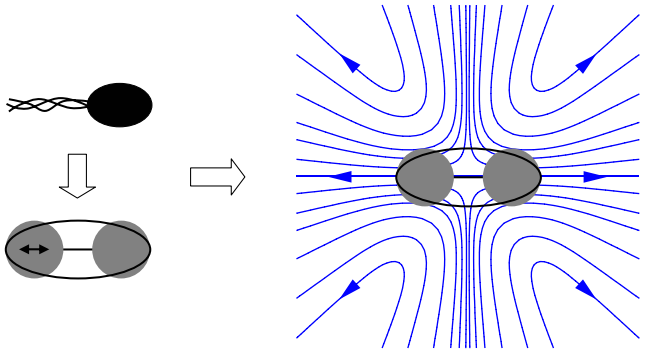

FIG. 1 (color online). Illustration of a pushing organism, swimmer model, and fluid disturbance they cause. The double arrow signifies the flagellum force acting on the bead and opposite force acting on the fluid, both acting at the center of the first bead. The blue (or dark gray) lines represent streamlines of the axisymmetric fluid disturbance. A puller produces the same streamlines with the arrows reversed.

cell whose flagella propel it forward predominantly from behind would be a pusher [19,25]. We shall see that this distinction is important. The swimmers also interact with an excluded volume potential using the repulsive portion of the Gay-Berne potential [26].

The motion of the swimmers is calculated by writing a force balance (neglecting inertia because of the small size of a microorganism) for each bead. On bead 1 of each swimmer this is $\mathbf{F}_f + \mathbf{F}_{h1} + \mathbf{F}_{c1} + \mathbf{F}_{e1} = \mathbf{0}$, where $\mathbf{F}_{h1}$ is the hydrodynamic drag force on the bead, $\mathbf{F}_{c1}$ is the connector (spring) force on the bead, and $\mathbf{F}_{e1}$ is the excluded volume force on the bead. On bead 2 of each swimmer the force balance is identical except without a flagellum force. The drag force is written using Stokes's law, $\mathbf{F}_{h1} = -6\pi\eta a[\dot{\mathbf{r}}_1 - \mathbf{v}'(\mathbf{r}_1)]$, where a is the bead radius, η is the fluid viscosity, $\mathbf{r}_1$ is the position of the bead, and $\mathbf{v}'(\mathbf{r}_1)$ is the fluid velocity at $\mathbf{r}_1$ generated by all other beads and phantom flagella. This fluid velocity is calculated using an order N method [27], treating each bead of the swimmer as a regularized point force. We set $\ell = 3a$. Note that the net force exerted by an isolated swimmer on the fluid is zero—overall, a neutrally buoyant swimmer is a force dipole to leading order. This model captures the universal far-field behavior while neglecting the near-field corrections to interactions between swimmers, which are dependent on the details of the organism. The validity of this approximation is supported by recent simulations [28]. Finally, we note that the limited set of results with multibead rod swimmers is qualitatively consistent with those for the two-bead swimmers.

The fluid motion generated by each swimmer perturbs the trajectories of fluid elements (tracers) and other swimmers. At the volume fractions considered here, this motion also eliminates any long-range orientational order among the swimmers. The motion of both tracers and swimmers, while ballistic at short times, becomes diffusive at long times. The tracer diffusion, in particular, shows important and unanticipated behavior. Figure 2 shows tracer mean-squared displacements (inset) and the long-time tracer diffusivity D_t in a suspension of pushers as a function of system size for $\phi_e = 0.1$. The diffusivity grows significantly with system size, greatly enhancing it beyond that for a suspension of pullers (also shown), which exhibits only weak or negligible system size dependence.

The system size dependence observed for pushers is due to collective behavior; simulations in which the swimmers do not interact, swimming in straight paths, do not show a significantly changing diffusivity. This observation has important implications for transport of nutrients, chemoattractants, and other chemical species in the environment of a population of swimming organisms. For example, organisms which concentrate toward an attractant will disperse that attractant more rapidly if they are pushers than if they are pullers. The remainder of this report describes efforts to gain an understanding of the increased transport.

The diffusivity is related to the fluid velocity through the Green-Kubo relation [29], $D_t = \frac{1}{3}\int_0^\infty \langle \mathbf{v}_t(0)\cdot\mathbf{v}_t(t)\rangle dt$, where $\mathbf{v}_t$ is the velocity of a tracer (fluid element) and angle brackets indicate an ensemble average. The mean-squared tracer velocity $\langle v_t^2\rangle = \langle \mathbf{v}_t(0)\cdot\mathbf{v}_t(0)\rangle$ is shown in Fig. 2 and has a much weaker system size dependence. The simple idea that the swimmer velocity is the isolated value

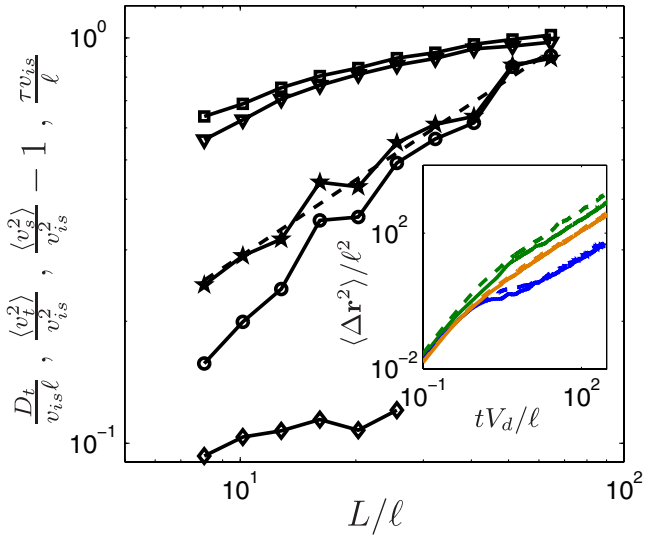

FIG. 2 (color online). System size dependence at volume fraction $\phi_e = 0.1$ for pushers. Variation of mean-squared tracer velocity $\langle v_t^2\rangle$ (squares), $\langle v_s^2\rangle - v_{is}^2$ (triangles), tracer diffusivity D_t (circles), and tracer correlation time (stars). The dashed line is a power law with $\alpha = 0.63$. The tracer diffusivity in a suspension of pullers is shown with diamonds. (inset) Tracer mean-squared displacements versus time for independent swimmers (blue or dark gray), pullers (orange or light gray), and pushers (green or gray) for $N = 400$ (solid) and $N = 3200$ (dashed). Averages over 400 tracers typically give statistically converged results.

plus the tracer velocity, $\mathbf{v}_s = \mathbf{v}_{is} + \mathbf{v}_t$, predicts that $\langle v_s^2 \rangle \approx v_{is}^2 + \langle v_t^2 \rangle$, which is verified in Fig. 2.

We now define a correlation time $\tau = D_t/\langle v_t^2 \rangle$ for the trajectories of tracer particles—tracer motion becomes diffusive on times $t \gg \tau$. Figure 2 shows τ versus L; over the entire range of system sizes considered, this relation displays a clear power law dependence $\tau \sim L^\alpha$, with $\alpha = 0.63 \pm 0.03$, over a range spanning a factor of 8 in L and thus 512 in N. These data represent the first examination of system size effects on the fluid response in swimming suspensions, and includes orders of magnitude more swimmers than any previous studies. For larger systems the behavior may transition to a non-power-law regime, but the system size dependence shown here will nevertheless cause significant enhancement of transport in a suspension of pushers.

The time τ represents the time a tracer moves in the same direction. A corresponding step length or correlation length l_t for the tracer's random walk scales as $\tau \langle v_t^2 \rangle^{1/2}$. Because $\langle v_t^2 \rangle$ has a much weaker dependence on L than τ, our results imply the existence of a correlation length for pushers that obeys $l_t \sim \ell(L/\ell)^\alpha \sim \ell^{(1-\alpha)} L^\alpha$ over the range of system sizes examined. The suspension of pushers leads to enhanced correlation lengths in the fluid, beyond pullers or independent swimmers, because of this increase with system size.

Before elaborating on correlation lengths, we briefly address the concentration dependence, using simple scaling arguments. In the Green-Kubo relation, the tracer velocity is a sum of disturbances due to each swimmer. Assuming independence of the swimmers in the dilute limit, the cross terms from the dot product vanish, resulting in $D_t \sim \phi_e$. For the same reason, $\langle v_t^2 \rangle \sim \phi_e$, which leads to a correlation time τ that is independent of volume fraction. Turning to swimmers rather than tracers, we note that in the dilute limit, the swimmers continue in straight lines until perturbed by other swimmers. If we define a cross section σ for these "collisions," the mean free path or step length l_s scales as $\ell^3/(\sigma \phi_e)$. Because $\langle v_s^2 \rangle \approx v_{is}^2 + \langle v_t^2 \rangle$ and $\langle v_t^2 \rangle \sim \phi_e$, the root-mean-squared swimmer velocity is $\langle v_s^2 \rangle^{1/2} \sim v_{is} + O(\phi_e)$. Therefore, the diffusivity scales as $D_s \sim \langle v_s^2 \rangle^{1/2} l_s \sim \phi_e^{-1}$. For $\phi_e \lesssim 10^{-2}$ simulation results follow these predictions (not shown), while above that volume fraction, they begin to deviate, indicating a breakdown of the assumption of independent swimmers.

We now return to the issue of correlation lengths, and consider the fluid velocity spatial correlation function, $C(\mathbf{r}) = \langle L^{-3} \int \mathbf{v}_t(\mathbf{r}') \cdot \mathbf{v}_t(\mathbf{r}' + \mathbf{r}) d\mathbf{r}' \rangle$. This is shown in Fig. 3 at a volume fraction of $\phi_e = 0.1$ for a range of system sizes. For independently distributed point dipoles, this correlation is $C_{id}(\mathbf{r}) = V_d^2 \ell / r$, where $V_d^2 = \phi_e d^2/(5\eta^2 \pi^2 \ell^4)$, and d is the dipole moment [30]. Because of the finite size of the swimmers and domain, real independent swimmers will deviate from this relation when $r \lesssim \ell$ or $r \approx L$. Even this simple result illustrates the possible complexities that arise in considering swimming suspensions; the velocity correlations are very long-ranged even in the absence of correlations between the positions and orientations of the swimmers.

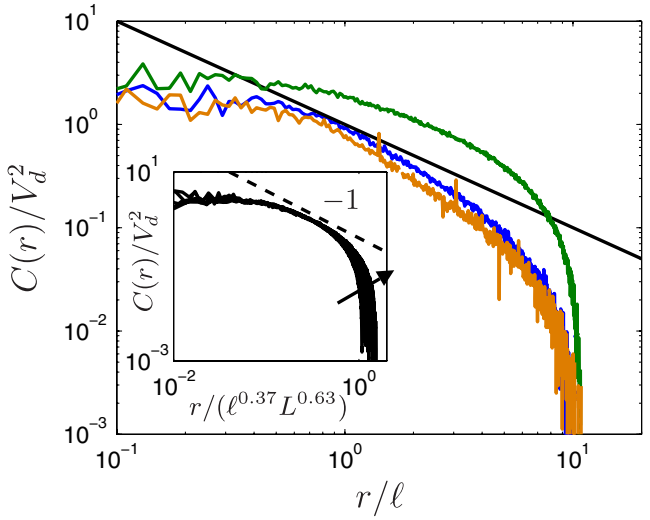

FIG. 3 (color online). The correlation function at $N = 3200$ for different models at $\phi_e = 0.1$: independent swimmers (blue or dark gray), independent point dipole theory (black), full simulation of pushers (green or gray), and pullers (orange or light gray). (inset) Correlation function for pushers at different system sizes with the spatial extent rescaled by $l_t = \ell^{0.37} L^{0.63}$. The arrow denotes increasing system sizes $N = 400 \rightarrow 6400$.

Figure 3 shows the correlation function at a characteristic system size of $N = 3200$ ($L = 25.589\ell$), for pushers, pullers, noninteracting pushers (where the swimmers do not feel the fluid motion but the tracer particles do) and the point dipole theory result. The noninteracting swimmer simulation shows the expected deviations from C_{id} at small r and large r due to the assumptions of the theory. For the interacting pushers, the tracer correlation is larger than that of the ideal theory and is system size-dependent as illustrated below, while for pullers, it remains close to that for independent swimmers, regardless of system size. The presence or absence of system size dependence in the velocity correlations is consistent with that for tracer diffusivity.

The connection between extended spatial correlations and the system size-dependent diffusivity for pushers is made clearer by returning to the system size-dependent correlation length l_t. The inset to Fig. 3 shows the velocity correlation function for pushers at $\phi_e = 0.1$ for several different system sizes with distance scaled by l_t. Except at distances close to the total box size, this scaling collapses the results to a single curve. This suggests that the correlation length inferred from the diffusivity also controls the spatial velocity correlations. At intermediate distances, the curves are consistent with a generalized point dipole theory, with a correlation of the form $C(r) \sim L^\alpha \ell^{(1-\alpha)}/r$.

The origin of the difference between pusher and puller dynamics is not completely clear, but a simple argument and some analysis can shed some light on the issue.

Imagine an initially homogeneous isotropic suspension of swimmers subject to a perturbation in the form of a shear flow. In a suspension of pullers, the shear flow distorts the orientation distribution and the resulting shear stress due to this distortion opposes the original shear flow, driving the system back to isotropy. This situation is closely analogous to a Brownian suspension of fibers or polymer molecules, the difference being that in the case of the swimmers the force dipoles that lead to the stress are intrinsic rather than induced by the shear. In the case of pushers, however, the initial shear flow distorts the orientation distribution in the same way, but now the force dipoles have opposite signs from the puller case and lead to a shear stress that *enhances* the original shear flow perturbation. This enhancement further increases the orientation of the swimmers, thus implying instability with respect to shear perturbations of the homogeneous isotropic state.

This argument can be made precise through a simple mean field theory (a related analysis without the above physical argument is given by [31]). Let $\mathbf{u} = \langle \mathbf{v}_t \rangle$ and $\boldsymbol{\alpha} = \langle \mathbf{nn} \rangle$, where $\mathbf{n}$ is the director vector of a swimmer. For a homogeneous isotropic state, the number density c is constant, $\mathbf{u} = \langle \mathbf{n} \rangle = 0$ and $\boldsymbol{\alpha} = \frac{1}{3}\boldsymbol{\delta}$. In the point dipole limit the stress tensor generated by the swimmers is $\boldsymbol{\tau}_s = dc\boldsymbol{\alpha}$, where d is the dipole strength per swimmer ($d > 0$ for pullers, $d < 0$ for pushers). Stokes's equation relates $\mathbf{u}$ and $\boldsymbol{\tau}_s$, and $\mathbf{n}$ evolves as would an infinitesimal material line subject to the constraint of constant length [32]. Considering linear stability of the homogeneous isotropic state subject to a shear flow disturbance $u_y(x)$ in the long-wave limit, Stokes's equation and the evolution equation for α_{xy} become $\eta \partial_x u_y = -dc\alpha_{xy}$ and $\partial_t \alpha_{xy} = (1/5)\partial_x u_y$. Combining these shows that α_{xy} evolves exponentially in time with growth rate $\sigma = -dc/5\eta$; for pullers, the shear perturbation decays, while for pushers it grows, confirming the simple physical argument given above. This result is wavelength independent in the long-wave limit and illustrates a mechanism for generating long-range correlations as seen in the full pusher simulations.

The qualitative differences we observe between pushers and pullers naturally leads to the question of whether different organisms have evolved their method of swimming partially based on how significantly that method of swimming enhances transport in the fluid. In addition to biological systems, a number of artificial microswimmers have recently been developed [33–37]. The impact shown here of the mode of swimming on collective behavior could be an important design criterion for future devices of this kind.

We gratefully acknowledge support from NSF Grants No. CTS-0522386 and No. DMR-0425880.

*Present address: Departamento de Materiales, Faculdad de Minas, Universidad Nacional de Colombia, Medellin, Carrera 80, #65-223, Bloque M3-050 Medellin, Colombia.

†Corresponding author.
graham@engr.wisc.edu

[1] E. Kunze *et al.*, Science **313**, 1768 (2006).
[2] A. W. Visser, Science **316**, 838 (2007).
[3] N. H. Mendelson *et al.*, J. Bacteriol. **181**, 600 (1999).
[4] X.-L. Wu and A. Libchaber, Phys. Rev. Lett. **84**, 3017 (2000).
[5] C. Dombrowski *et al.*, Phys. Rev. Lett. **93**, 098103 (2004).
[6] I. H. Riedel, K. Kruse, and J. Howard, Science **309**, 300 (2005).
[7] A. Sokolov *et al.*, Phys. Rev. Lett. **98**, 158102 (2007).
[8] M. J. Kim and K. S. Breuer, Phys. Fluids **16**, L78 (2004).
[9] T. Vicsek *et al.*, Phys. Rev. Lett. **75**, 1226 (1995).
[10] R. A. Simha and S. Ramaswamy, Phys. Rev. Lett. **89**, 058101 (2002).
[11] K. Kruse *et al.*, Phys. Rev. Lett. **92**, 078101 (2004).
[12] I. S. Aranson *et al.*, Phys. Rev. E **75**, 040901(R)(2007).
[13] G. I. Taylor, Proc. R. Soc. A **209**, 447 (1951).
[14] J. Lighthill, SIAM Rev. **18**, 161 (1976).
[15] E. M. Purcell, Am. J. Phys. **45**, 3 (1977).
[16] S. Nasseri and N. Phan-Thien, Comput. Mech. **20**, 551 (1997).
[17] T. Ishikawa, M. P. Simmonds, and T. J. Pedley, J. Fluid Mech. **568**, 119 (2006).
[18] T. Ishikawa *et al.*, Biophys. J. **93**, 2217 (2007).
[19] J. P. Hernandez-Ortiz, C. G. Stoltz, and M. D. Graham, Phys. Rev. Lett. **95**, 204501 (2005).
[20] C. Stoltz, Ph.D. thesis, UW-Madison, 2006.
[21] I. Llopis and I. Pagonabarraga, Europhys. Lett. **75**, 999 (2006).
[22] D. Saintillan and M. J. Shelley, Phys. Rev. Lett. **99**, 058102 (2007).
[23] T. Ishikawa and T. J. Pedley, J. Fluid Mech. **588**, 399 (2007).
[24] T. Ishikawa and T. J. Pedley, J. Fluid Mech. **588**, 437 (2007).
[25] D. Bray, *Cell Movements: From Molecules to Motility* (Garland, New York, 2001), 2nd ed.
[26] M. Allen and G. Germano, Mol. Phys. **104**, 3225 (2006).
[27] J. P. Hernandez-Ortiz, J. J. de Pablo, and M. D. Graham, Phys. Rev. Lett. **98**, 140602 (2007).
[28] V. Mehandia and P. Nott, J. Fluid Mech. **595**, 239 (2008).
[29] D. McQuarrie, *Statistical Mechanics* (Harper Collins, New York, 1976).
[30] Our independent dipole theory gives a mean-squared tracer velocity $\langle v_t^2 \rangle = C(0) \sim (2\phi_e d^2 k_{\mathrm{cut}})/(5\eta^2\pi^3\ell^3)$, where $k_{\mathrm{cut}} \approx 2\pi/\ell$ represents the characteristic wave vector beyond which the point dipole theory is regularized.
[31] D. Saintillan and M. J. Shelley, Phys. Rev. Lett. **100**, 178103 (2008).
[32] R. B. Bird, C. F. Curtiss, R. C. Armstrong, and O. Hassager, *Dynamics of Polymeric Liquids*, Kinetic Theory Vol. 2 (Wiley, New York, 1987), 2nd ed..
[33] R. Ismagilov *et al.*, Angew. Chem., Int. Ed. **41**, 652 (2002).
[34] R. Golestanian, T. B. Liverpool, and A. Ajdari, Phys. Rev. Lett. **94**, 220801 (2005).
[35] R. Dreyfus *et al.*, Nature (London) **437**, 862 (2005).
[36] W. Paxton *et al.*, Angew. Chem., Int. Ed. **45**, 5420 (2006).
[37] T. Hogg, Auton. Agents Multi-Agent Syst. **14**, 271 (2007).